



ELSEVIER

Geoderma 70 (1996) 133–163

GEODERMA

Physics of gravity fingering of immiscible fluids within porous media: An overview of current understanding and selected complicating factors

R.J. Glass, M.J. Nicholl

Geohydrology Department 6115, Sandia National Laboratories, Albuquerque, NM 87185-1324, USA

Received 1 October 1994; accepted 23 February 1995

Abstract

While gravity fingering of water in unsaturated sands has been demonstrated and studied under constrained laboratory conditions, its significance under field conditions in the vadose zone is still under debate. We review current understanding of the gravity fingering process as developed through linear stability analysis and laboratory experiments. With respect to many complicating factors inherent in the field, this understanding is deficient in determining the field conditions where gravity fingering can be expected and the behavior of the field-scale fingering process when it occurs. This deficiency is exemplified in the results we present of a field experiment conducted in a sandy alluvial deposit. While simple extrapolation of current understanding of the process predicted instability, fingers did not occur. To begin to understand the influence of complicating factors inherent in the field, we conducted several laboratory experiments that address three important complicating factors: uniform and non-uniform initial moisture content, media heterogeneity, and the presence of macropores and fractures. These factors can fundamentally alter the gravity fingering process, its scale of expression and, under many field conditions, suppress its occurrence entirely. While the significance of gravity fingering of water in a wettable vadose zone is still inconclusive, gravity fingering will likely play a significant role in water/NAPL (non-aqueous-phase liquid) or water/NAPL/air systems, as occur within the saturated and vadose zones, respectively, at many contaminated industrial sites. To demonstrate this role, the results of a simple experiment are presented.

1. Introduction

Current physical understanding of gravity-driven water fingering instigated from wetting front instability in unsaturated porous media has been developed primarily through mathematical analysis and laboratory experimentation. Stability criteria, and

relations for finger width or diameter formulated through linear stability analysis in both two- and three-dimensional systems have been compared to laboratory experiments in initially dry, water-wettable sands. While linear stability theory allows first-order insight into the interplay of gravitational, viscous, and capillary forces in stabilizing or destabilizing flow fields, it neither predicts nor explains many significant features observed in laboratory experiments; finger velocity, finger-moisture-content structure, the number of fingers that form, and finger persistence in time and space are some of the observed phenomena unaccounted for by linear stability theory. Laboratory experiments that yield this data are, however, limited in that only a narrow range of parameter space within very homogeneous sand packs has been interrogated.

Due to the great distance between current understanding (analytical and laboratory) and the complicated conditions inherent in the field, application of results from linear analysis or laboratory experimentation to the field must be made with caution. Complicating factors inherent in field soils include the effects of uniform and non-uniform initial moisture content, media heterogeneity, macropores and fractures, and media hydraulic/capillary properties. It may be possible to treat one or more of these factors through the definition of equivalent effective media properties, which in turn would be incorporated into existing functional relations to account for finger behavior. Alternatively, these factors may act to fundamentally alter the fingering process, its scale of expression, or suppress its occurrence entirely.

In this paper, we summarize current understanding of gravity fingering derived from: (1) theory as developed through linear stability analysis; and (2) laboratory experiments conducted in homogeneous, water wettable sands. We then present the results of a field experiment, followed by laboratory experiments, that consider the complicating effects of uniform and non-uniform initial moisture content, media heterogeneity, and the presence of macropores and fractures. Media hydraulic/capillary properties are discussed from a pore scale perspective elsewhere in this issue (Glass and Yarrington, 1996). Finally, we briefly discuss the parallel problem of gravity fingering during non-aqueous-phase liquid (NAPL) transport in the subsurface.

2. Theory developed through linear stability analysis

The interplay of viscous and gravitational forces in determining the stability of an advancing sharp front separating two immiscible fluids within a porous medium in the absence of capillary forces was developed independently through linear stability analysis by Saffman and Taylor (1958) and Chouke et al. (1959). This interplay is captured in the following expression:

$$kg \cos \beta (\rho_1 - \rho_2) - \theta_a U (\mu_1 - \mu_2) < 0 \quad (1)$$

where k is the intrinsic permeability of the media, g is the gravitational acceleration, β is the angle between the gravitational vector and the direction of flow, θ_a is the porosity of the media, U is the interfacial velocity in the direction of flow, ρ_1 and ρ_2 are the densities of the upstream and downstream fluids, respectively, μ_1 and μ_2 are the viscosities of the upstream and downstream fluids, respectively.

Table 1
Classification of gravitational and viscous effects on fluid–fluid displacement

	Gravity stabilized	Gravity destabilized
Viscous stabilized	Type I — unconditionally stable fluid accelerated upward/downward into a less/more dense, less viscous fluid	Type II — conditionally unstable fluid accelerated downward/upward into a less/more dense, less viscous fluid
Viscous destabilized	Type III — conditionally unstable fluid accelerated upward/downward into a less/more dense, more viscous fluid	Type IV — unconditionally unstable fluid accelerated downward/upward into a less/more dense, more viscous fluid

When the inequality (1) is satisfied, stability is predicted; otherwise, any perturbation (finite or infinitesimal) to the interface between the two immiscible fluids will grow to dominate the displacement process. Table 1 displays the four categories (I, II, III, IV) of behavior that exist with respect to the combined influence of viscous and gravitational forces on interfacial stabilization or destabilization. Within the context of the air/water system where air is the less dense, less viscous fluid, these four categories are exemplified respectively by: Category I, a rising water table; Category II, the surface infiltration of water into an air filled soil; Category III, air injection into the top of a water saturated soil column where water (and air) can escape out the bottom of the column; and Category IV, air injection below the water table.

For many situations in vadose zone hydrology or soil science, gravity instability within category II is suggested by the linear theory. Neglecting the viscosity and density of air with respect to those of water, the Saffman–Taylor/Chouke stability criterion reduces to:

$$\theta_a U > \frac{kg\rho_1}{\mu_1} \text{ or } q_s > K_s \quad (2)$$

where q_s is the flux through the system and K_s is the saturated conductivity of the porous medium. Thus, any time the downward water flux is less than the saturated conductivity of the porous medium (i.e., gravitational destabilizing forces overwhelm viscous stabilizing forces), instability is predicted. Examples of this situation are widespread, and include: infiltration through layered systems where a layer of lower K_s overlies one with a higher K_s , redistribution following ponded infiltration within a single layer, and uniformly distributed water application to a single layer at a flux less than K_s by rainfall, irrigation, or through a porous plate (as in a laboratory column experiment).

Capillary forces along the fluid/fluid interface are neglected in the derivation of Eq. (1). However, such forces are almost always non-negligible with respect to gravitational and viscous forces and thus should also be included in the stability analysis. The linear analysis of Chouke et al. (1959) included capillary forces in the form of an effective surface tension (σ_*) at the macroscopic interface (above the pore scale). Parlange and Hill (1976) conducted a linear stability analysis that considered capillary forces as

parameterized by the soil water sorptivity (S). Using either approach to include capillarity, system stability is predicted through the interplay of viscous, gravitational, and capillary forces. Capillary forces act to stabilize perturbations to the front below a critical wavelength. Assuming that finger width or diameter is predicted by half this wavelength, a minimum finger size (d_c) is predicted for a particular porous medium and applied flux. Following both approaches, d_c is given by:

$$d_c = \alpha \sqrt{\sigma_* k} \left(\frac{1}{U\theta_s(\mu_2 - \mu_1) + kg(\rho_1 - \rho_2)} \right)^{1/2} \quad (3)$$

for Chouke et al. (1959) and:

$$d_c = \alpha \frac{S^2(\mu_1 + \mu_2)}{2(\theta_s - \theta_i)} \left(\frac{1}{U\theta_s(\mu_2 - \mu_1) + kg(\rho_1 - \rho_2)} \right) \quad (4)$$

for Parlange and Hill (1976). S is the sorptivity evaluated between θ_s and θ_i , θ_s is the saturated moisture content, θ_i is the initial moisture content, and α is a constant equal to π for a two-dimensional system and 4.8 for a three-dimensional system (Glass et al., 1991b).

Specialization of Eqs. (3) and (4) to the air/water system where the density and viscosity of air are negligible with respect to those of water, and defining a dimensionless system flux ratio ($R_s = q_s/K_s$) leads to the following simplifications:

$$d_c = \alpha \sqrt{\frac{\sigma_*}{\rho g}} \left(\frac{1}{1 - R_s} \right)^{1/2} \quad (5)$$

for Chouke et al. (1959) and:

$$d_c = \alpha \frac{S^2}{2K_s(\theta_s - \theta_i)} \left(\frac{1}{1 - R_s} \right) \quad (6)$$

for Parlange and Hill (1976).

Eqs. (5) and (6) are a product of two terms. The first, preceding the bracket, is a length scale defined by the ratio of capillary to gravitational forces. Within the bracket is a dimensionless function that describes the relative importance of viscous and gravitational forces. At small flow rates R_s approaches zero, indicating the dominance of gravitational forces over viscous forces; d_c is then given by the ratio of capillary to gravitational forces. The stability criterion of Eq. (2), weighing viscous to gravitational forces, is contained within Eqs. (5) and (6) in the system parameter R_s . For high flow rates, d_c becomes infinite as R_s approaches 1; viscous forces dominate both gravitational and capillary forces. If the horizontal extent of the system falls below d_c , then the system will be filled with one finger and stability is forced. Thus, for a given porous medium and applied flux at less than K_s , the stability of a system depends on its horizontal extent, as capillary forces stabilize all systems smaller than d_c .

Inclusion of capillary forces also allows us to develop relationships for an expected finger width/diameter (d) as a function of viscous, gravitational, and capillary forces. Through extremization of the growth rate with respect to perturbation wavelength, and

again assuming that half this wavelength yields the expected finger width/diameter, we obtain:

$$d = \alpha \sqrt{3\sigma_*} k \left(\frac{1}{U\theta_s(\mu_2 - \mu_1) + kg(\rho_1 - \rho_2)} \right)^{1/2} \quad (7)$$

for Chouke et al. (1959) and:

$$d = \alpha \frac{S^2(\mu_1 + \mu_2)}{(\theta_s - \theta_i)} \left(\frac{1}{U\theta_s(\mu_2 - \mu_1) + kg(\rho_1 - \rho_2)} \right) \quad (8)$$

for Parlange and Hill (1976) or for the air/water system where the density and viscosity of air are negligible with respect to those of water:

$$d = \alpha \sqrt{\frac{3\sigma_*}{\rho g}} \left(\frac{1}{1 - R_s} \right)^{1/2} \quad (9)$$

for Chouke et al. (1959) and:

$$d = \alpha \frac{S^2}{K_s(\theta_s - \theta_i)} \left(\frac{1}{1 - R_s} \right) \quad (10)$$

for Parlange and Hill (1976).

Comparison of these relations for finger width to that obtained in two-dimensional experiments is discussed below in Section 3.2.

3. Observations from laboratory experiments in water wettable sands

Gravity finger formation during vertical infiltration in layered soils was encountered by a number of early researchers (e.g., Palmquist and Johnson, 1960, 1962; Tabuchi, 1961; Peck, 1965). However, the first experimental investigation directed at gravity fingering in initially dry, water-wettable porous media was that of Hill and Parlange (1972) who constructed a series of experiments within the context of a two-layer (fine over coarse) system (Category II). Gravity fingering was demonstrated and discussed with respect to the Saffman–Taylor/Chouke stability criterion (Eq. 2). Diment and Watson (1985) considered stability with respect to redistribution following ponded water application. In a series of experiments, they showed that instability occurred immediately after infiltration, provided that the infiltration volume was sufficient to allow redistribution. Infiltration from rainfall into a single layer at a rate less than K_s is also predicted to be unstable by Eq. (2); Selker et al. (1992c) demonstrated this condition to be nearly identical to the two-layer case.

Observations from laboratory experiments following the onset of instability have allowed us to both test the predictions of linear stability theory for finger width/diameter and to discover a number of unexpected features of fingering flow fields. The most important features have been visualized by newly developed techniques allowing measurement of two-dimensional saturation fields (Glass et al., 1989d; Tidwell and

Glass, 1994) (see Fig. 1). From such data, it is seen that the fingering process in water-over-air systems is characterized by two distinct time scales, one for the rapid downward growth of fingers and a second, much longer time scale associated with the slow lateral diffusion of water from the finger into the surrounding dry media. Below, we summarize current understanding of both rapid and long-term flow field development. We then present relations measured for finger width/diameter and finger velocity. Scaling of these relations to allow the generalization of results to other geometrically similar porous media and fluid/fluid systems is then discussed.

3.1. Finger structure and long-term flow field development

Typical finger moisture content structure during the rapid growth stage is shown in Fig. 1. As a finger grows downward from the textural interface under low supply rates, the finger tip wets to near saturation for the media. At a distance behind the advancing tip, the finger begins to desaturate. If constant flow to the finger continues, the relative

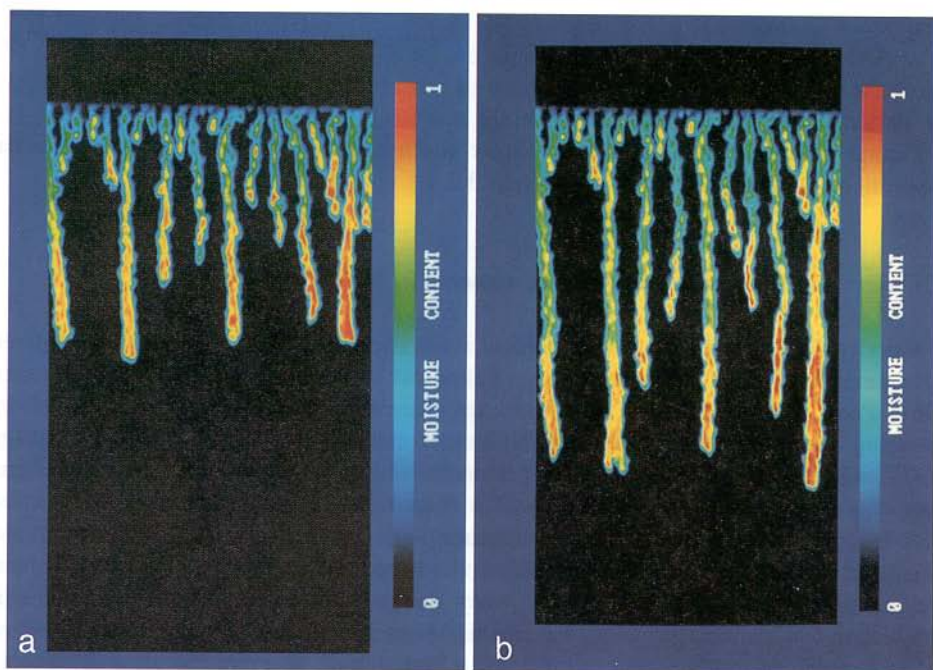


Fig. 1. Finger formation during rapid growth stage. The downward growth of fingers in an initially dry porous medium is shown in a sequence of two images using the light transmission technique to capture saturation fields (from Glass et al., 1989d). The total flux through the system is controlled by a thin top layer of lower conductivity (dark rectangle at top) which uniformly supplies water to the underlying layer at an R_s of 0.1. Fingers form in the higher conductivity medium directly below the top layer. The dimensions of the higher conductivity medium are 45 cm wide, 76 cm high and 1 cm thick (into the plane of the experiment). If the thickness of the medium is less than the minimum finger width, a two-dimensional flow field is forced, as is the case here.

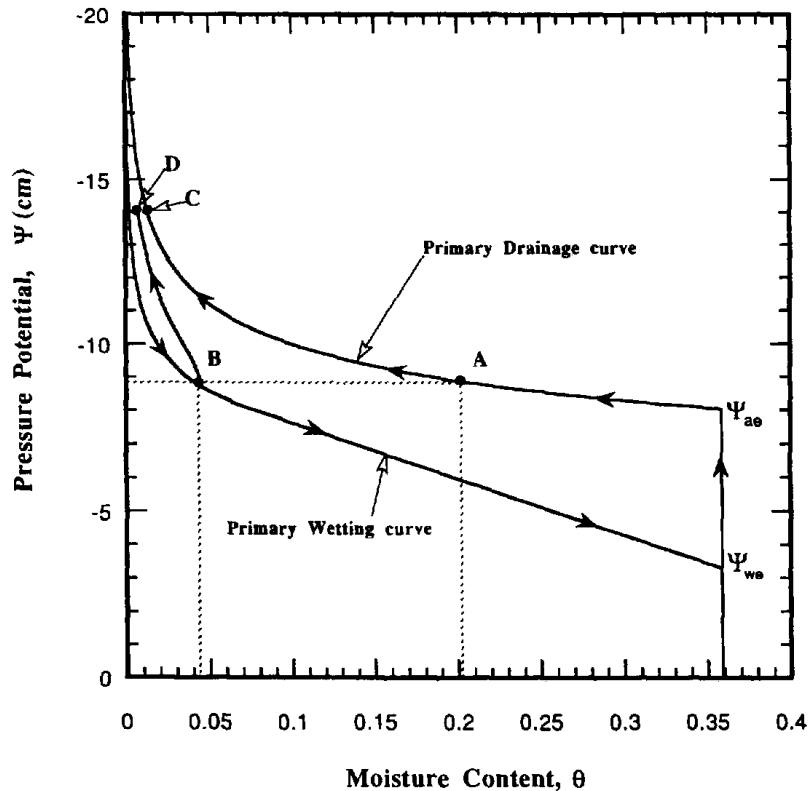


Fig. 2. Hysteretic moisture characteristic curves. Primary wetting and drainage curves are shown for a typical narrow grain size distribution sand (14–20 mesh) as calculated using the theory of Hogarth et al. (1988) from the measured primary drainage curve. Point A represents the pressure potential – moisture content after the finger tip passes and from which the fringe develops to pressure equilibrium at point B. Following interruption of flow and subsequent drainage of the field, the core and fringe moisture contents remain distinct at points C and D, respectively, as they follow different drainage curves (see Glass et al., 1989d).

permeability and supply flux under unit gradient conditions will combine to determine moisture content within the desaturated region.

The development of a saturated tip, and the subsequent drainage behind the tip may be understood by considering the saturated tip as a short hanging water column of length L_s . The wetting and drainage curves for the media (see Fig. 2) yield the pressure potentials at which the sand will wet at the finger tip (the water entry value ψ_{we}) or begin to drain at the rear (the air entry value ψ_{ae}). At low flow rates, viscous forces can be neglected; once L_s is longer than the difference between ψ_{we} and ψ_{ae} , the hanging column of the tip exerts enough suction to desaturate the finger above. Experimentally, L_s , finger velocity, and moisture content in the desaturated zone are all found to be increasing functions of flow rate supplied to the finger. Using simple arguments, a relationship for L_s as a function of the flux through the finger (q_f) and hydraulic properties was developed by Glass et al. (1989d):

$$L_s = \frac{\psi_{we} - \psi_{ae}}{1 - R_f} \quad (11)$$

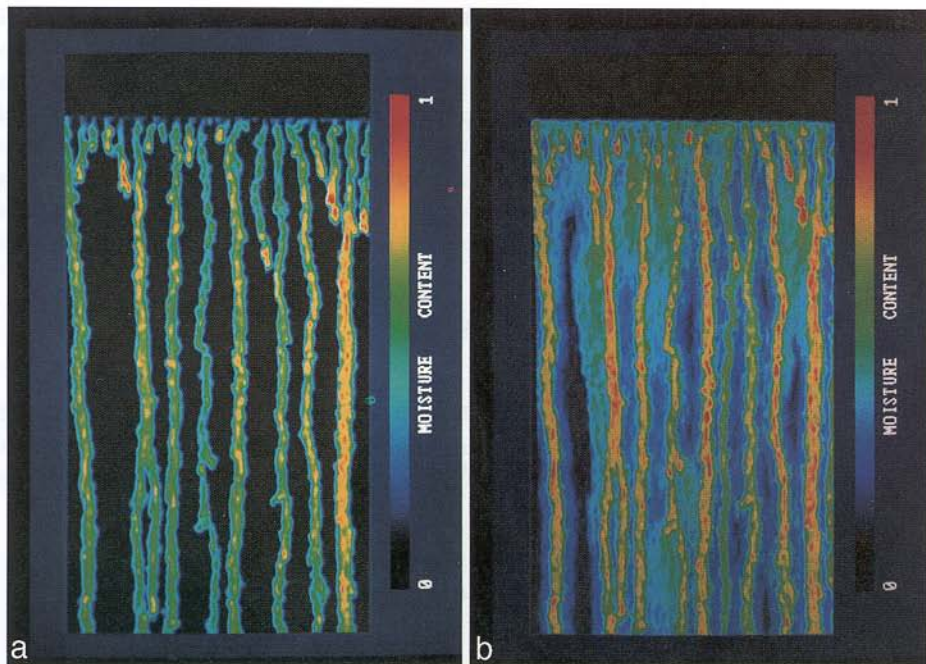


Fig. 3. Development of two-zone, core-fringe region during slow growth stage. The saturation field for the experiment in Fig. 2 is shown after one hour (a) and after 14 days (b) of continuous infiltration (from Glass et al., 1989d). Over this period, slow lateral movement of moisture from finger core regions creates a less saturated surrounding fringe region.

where R_f is the finger flux ratio given by q_f/K_s that describes the local ratio of viscous to gravitational forces and is analogous to the system scale, R_s , introduced earlier. Note that viscous forces modify the pressure potential within the saturated tip from hydrostatic such that as the flow rate increases, the saturated tip becomes longer before the pressure potential at the top decreases below the air entry value and drainage occurs. This simple effect of viscous forces on saturated tip length is supported by the experimental data of Liu et al. (1991). Additional verification of the hanging column model of a finger tip has been accomplished through the use of tensiometers to monitor pressure history at the textural interface (Baker and Hillel, 1990) and at a point during finger passage (Selker et al., 1992a). Selker et al. (1992b) were also able to predict the moisture content structure above the saturated tip by assuming a constant finger velocity.

Once fingers have formed and moved through a two-layer system, a constant steady supply of water over long periods of time results in the slow lateral movement of an unsaturated front from the original finger "core" regions (Fig. 3). The moisture content of this developing "fringe" region is much less than that in the core region. Eventually, nearly all the dry porous media between the fingers is wet at this low moisture content, producing a steady-state two-region moisture content field that persists in time. The development and persistence of this two-region structure is understood with respect to the hysteretic primary wetting and drainage curves shown in Fig. 2. Because the core

region is on the drainage curve and the fringe region is on the wetting curve, at pressure equilibrium a two-region moisture content field will result and persist (Glass et al., 1989d).

The spread of the fringe region has been shown to exhibit square root of time dependence (Glass et al., 1987). The primary mechanism for fringe region development is most likely a combination of film flow along the surfaces of grains and possibly vapor transport, as opposed to the pore filling which occurs in the rapid phase. Assuming constant surface chemistry and micro-roughness, the time scale of the film flow process should scale inversely with the surface area of the material per unit length of porous media, causing the rate of spread of the fringe region to increase with the mean grain size. In addition, contact points between grains should inhibit film flow, causing an additional increase in the time scale for the film flow process as the granular media becomes finer. In the experiments of Glass et al. (1989b,d), full development of the core/fringe structure took 1 day for the 14–20 (US sieve series) sand and about two weeks for the 20–30 sand, supporting this hypothesis.

As the final two-zone moisture content field is evolving, secondary fingers or “dendrites” may form at finger merger points, kinks in the original finger, or the base of lobes in the fringe region. Localized high pressure (low suction) may be associated with such structural features, thereby causing pore filling within the dry sand. If such pore filling creates a hanging column of length greater than $\psi_{we} - \psi_{ae}$ a dendrite will form. An example of a dendrite formed from a finger merger point is seen in Fig. 3b where an additional core region has grown between the third and fourth finger from the right in Fig. 3a. In this particular case, a slow moving finger contacted a faster, adjacent finger during the initial fingering stage and merged with it. During the spreading stage, pore filling below the merger point led to the formation of a dendrite. Such dendrites have only been found to form through dry sand where water can be supplied at a rate above what the film flow mechanism can remove.

3.2. Finger width / diameter and velocity

Relationships for the finger width/diameter (d) and finger velocity (v) as functions of porous media properties and finger fluxes (q_f) were developed for two-dimensional finger width (Glass et al., 1989b,c) and three-dimensional finger diameter (Glass et al., 1990) through a combination of dimensional analysis and systematic experimentation. System fluxes in two-layer cases were prescribed by the permeability of the top layer. Fluxes through individual fingers were calculated from average individual finger widths/diameters and individual finger flow rates measured out the bottom of the chamber through a specially designed manifold. In single-layer cases, point sources were imposed directly at the top of the layer to form an individual finger with precisely known supplied flow rate. For both types of experiment and in both two- and three-dimensional systems, d and v were found to follow:

$$d = \frac{\alpha S^2}{K_s(\theta_s - \theta_i)} \left(\frac{1}{1 - R_f} \right)^\gamma \quad (12)$$

where $\gamma = 1$ for finger width (2-D) and $1/2$ for finger diameter (3-D) and:

$$\nu = \frac{K_s}{(\theta_s - \theta_i)} [C + R_f(1 - C)] \quad (13)$$

where C is the projected zero flow velocity for fingers, determined experimentally to be 0.1 for two-dimensional systems and 0.23 for three-dimensional systems. Eq. (13) demonstrates that fingers move faster than expected because they desaturate behind their tips. Also note that because a zero flow velocity has no physical meaning, the constant C is only useful in the range where finger velocity was measured, $0.1 < R_f < 0.9$ (two-dimensional) and $0.03 < R_f < 0.94$ (three-dimensional).

For the two-dimensional system where many full-field instability experiments were conducted, a relationship between \bar{R}_f (the average R_f) and R_s at the system scale was observed for the range ($0.007 < R_s < 0.82$). Noting that R_s and \bar{R}_f are related by the fractional cross sectional area in fingers, $1/\beta$:

$$R_s = \bar{R}_f / \beta \quad (14)$$

analysis of two-dimensional system data yielded the relationship:

$$\bar{R}_f = \sqrt{R_s} \quad (15)$$

allowing Eqs. (12) and (13) to be written at the system scale for average width (\bar{d}) and velocity ($\bar{\nu}$):

$$\bar{d} = \frac{\alpha S^2}{K_s(\theta_s - \theta_i)} \left(\frac{1}{1 - \sqrt{R_s}} \right) \quad (16)$$

and:

$$\bar{\nu} = \frac{K_s}{(\theta_s - \theta_i)} (C + \sqrt{R_s}(1 - C)) \quad (17)$$

It must be recognized that these relationships were developed by Glass et al. (1989c,1990) within a specific range of R_f ($0.1 < R_f < 0.9$) and R_s ($0.007 < R_s < 0.82$) and for only one narrow grain sized distribution sand (14–20 mesh) in an initially dry condition. Furthermore, the sand packs were devoid of heterogeneity at the scale of observed fingers. Extrapolation of these results (especially Eq. 15) to other materials with different heterogeneity structures and imposed boundary/initial conditions must, therefore, be made with caution.

The functional form relating gravitational and viscous forces contained in Eq. (16) is different from either of the forms given by linear stability theory in Eqs. (9) and (10) (see Fig. 4). If we assume the fingers are unsaturated and replace $k\rho g/\mu$ by the average finger flux (q_f) as done by Glass et al. (1989c,1991a,b) and if the experimental result of Eq. (15) is used, then the linear theory of Parlange and Hill (1976) collapses to Eq. (16). Continued evidence, however, shows that during the initial development of fingers at textural interfaces, from applied rainfall (Selker et al., 1992c), or from point sources, fingers along the front are near saturation and very likely at the ‘‘satiated’’ (air entrapped) value of the moisture content. Therefore, the relevant condition for the linear

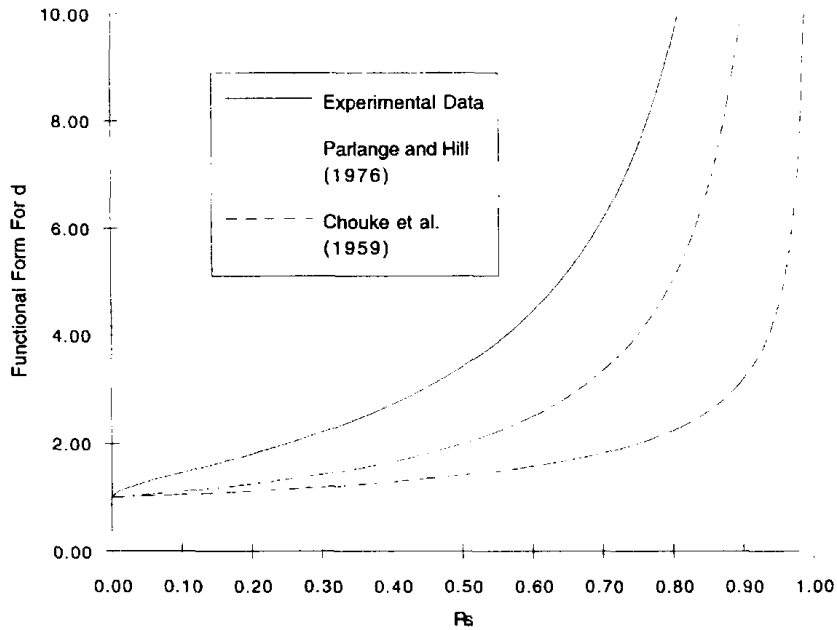


Fig. 4. Comparison of Eqs. (9) and (10) for finger width derived through linear stability theory to Eq. (16) which represents the experimental data.

stability analysis is a nearly saturated media and not the later time flux through the desaturated cores. The fact that linear theory does not predict accurately the width of fully developed fingers is not unexpected. Linear theory implicitly assumes infinitesimal perturbations to a flat front, which differs significantly from a fully developed finger.

3.3. Scaling of finger behavior in geometrically similar homogeneous media

Glass et al. (1989b) used capillary scaling theory incorporating both a microscopic and macroscopic length scale (see Miller and Miller, 1956) to build generalized forms of the relations for finger width and velocity. The dimensionless finger width/diameter (d_*) and dimensionless finger velocity (v_*) are given by:

$$d_* = \alpha \frac{S_*^2}{K_s \cdot (\theta_s - \theta_i)} \left(\frac{1}{1 - R_f} \right)^\gamma \tag{18}$$

and:

$$v_* = \frac{K_s \cdot}{(\theta_s - \theta_i)} [C + R_f(1 - C)] \tag{19}$$

where:

$$d_* = \frac{\rho g m}{\sigma} d \tag{20}$$

$$v_* = \frac{\mu}{\rho g m^2} v \quad (21)$$

$$K_{s*} = \frac{\mu}{\rho g m^2} K_s \quad (22)$$

$$S_*^2 = \frac{\mu}{\sigma m} S^2 \quad (23)$$

where σ is the surface tension of the fluid/fluid interface and m is a microscopic length scale taken as the mean grain size of the granular material.

For this theory to apply, the media must exhibit statistically similar geometries. This means that grain size distributions of the relevant media must be similar (differ by a multiplicative scale factor) and the porosities identical. In addition, as currently formulated, the theory does not apply for systems where forces other than viscous, capillary, and gravitational induce flow (e.g., in extremely small pores where flow may result from electrochemical forces).

Theory implies that for constant R_f , finger width should increase ($dm = \text{constant}$) and finger velocity should decrease ($v/m^2 = \text{constant}$) as m of the geometrically similar sand decreases. The effects of fluid properties and capillary/hydraulic properties on finger width and velocity can also be predicted in the dimensionless forms as long as the viscosity and density differences remain large enough for 16 and 17 to be valid (i.e., that the density and viscosity of the displacing fluid is much greater than those of the displaced fluid).

A small set of two-dimensional experiments within three narrow grain size distribution sands were reported by Glass (1992) and in Parlange et al. (1990) that suggest the scaling theory applies. Subsequently, Glass et al. (1991a) presented a more extensive series of two-dimensional experiments conducted in six geometrically similar sands where the mean grain size was varied over nearly an order of magnitude. For each of the sands, the scaled fluxes applied to the individual fingers also spanned almost an order of magnitude. The data confirmed the scaled functional forms for width and velocity in this particular family of similar sands over the ranges considered. However, in order to generalize scaling behavior to other dissimilar families, the grain size distribution about the mean, as well as the mean must be varied systematically.

4. Complicating factors

While a great deal has been learned from the laboratory experiments discussed above, most of these experiments have been conducted within a narrow range of parameter space: homogeneous, initially dry sands with narrow grain size distribution and large mean grain size at system flux ratios (R_s) above 0.01. To demonstrate the disconnect between current understanding (theory and laboratory) and application to field studies, we performed a simple field experiment within the sandy ancestral Rio Grande alluvial deposits in Albuquerque, NM (Martin et al., 1993). The deposit contains a number of well, to poorly sorted, hydrophilic layers. Photographs of the deposit (Fig. 5) show the



Fig. 5. Naturally occurring micro-layering and cross-bedding. Intermediate (top) and small (bottom) scale photographs of near surface alluvial deposit in Ancestral Rio Grande sediments, Albuquerque, NM. Flagging is on a 40 cm grid.

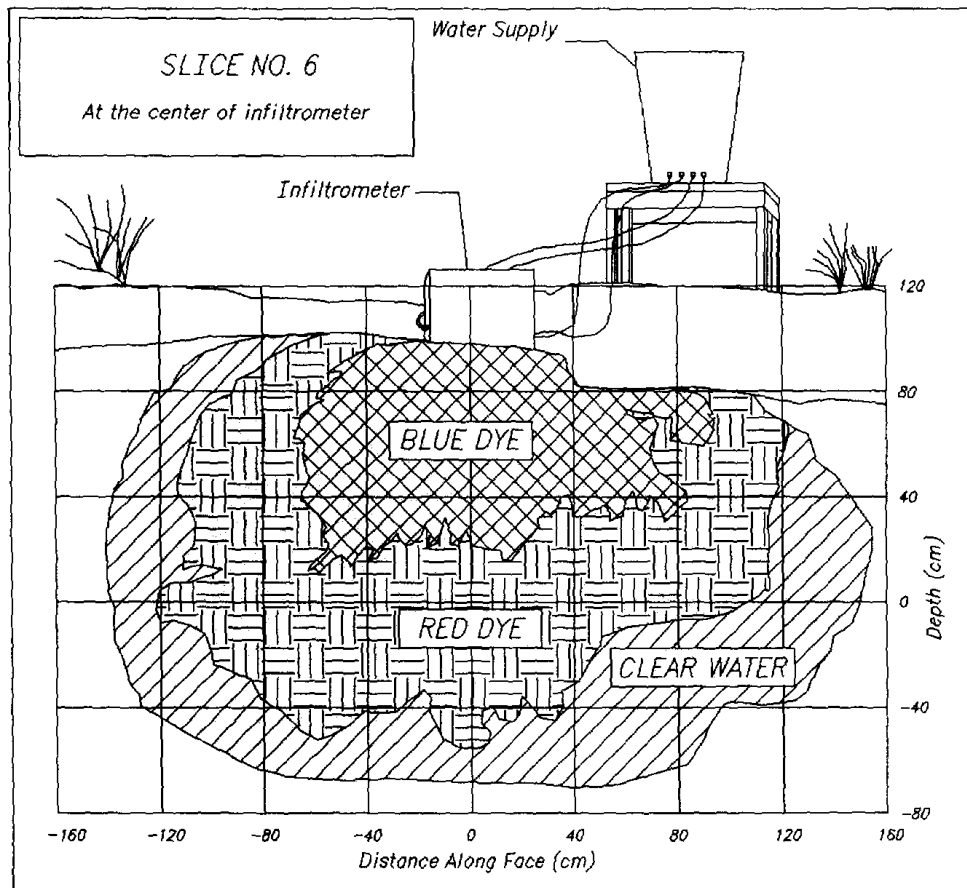


Fig. 6. Field experiment in complicated alluvial deposit. Water, red dye, and blue dye interfaces are shown for a vertical section under the midpoint of the infiltrometer. While theory predicts gravity fingering to occur, the wetting front remained stable. Preferential flow resulting from other mechanisms can be seen in the dye fronts behind the wetting front.

naturally occurring micro-layering and cross-bedding commonly found within subsurface field soils. At the top of this outcrop, a partially cemented fine sand approximately 30 cm thick created a permeability contrast of nearly an order of magnitude with underlying units. The near surface zone at the top of the outcrop was leveled to reduce the thickness of this lower permeability layer to approximately 10 cm and provide a flat, horizontal surface for water infiltration. Water containing first red, and then blue dye was ponded in a 45 by 45 cm zone at the top of the outcrop located 30 cm back from the outcrop face. Photographs of the outcrop face were taken to document the surficial expression of wetting and dye fronts as the experiment progressed. The organic dye used (food coloring) was observed to partition from the infiltration fluid; as a result, three distinct fronts were observed: wetting, red, and blue. After 240 gallons of water had infiltrated, the outcrop face was cut back into the formation to the midpoint of the ponded zone. Fig. 6 shows an outline of the wetting, red, and blue fronts on the cutback face. The wetting front was notably more uniform than either of the red or blue fronts. The root cause of irregularities in the dye fronts is difficult to determine and could result

from the lack of smoothing by capillarity forces, heterogeneity induced channeling, or differential adsorption of the dye. The dramatic finger structure as seen in laboratory experiments was certainly not evident, even though flux rates supplied to the lower layers were much less than their saturated conductivities.

A number of possibilities exist to explain the suppression of fingering during the field experiment, including: non-zero initial moisture content; media heterogeneity, (e.g., within layer micro-layering and cross-bedding); height of macroscopic layers; and the hydraulic/capillary properties of the layers. In order to more confidently apply laboratory and theoretical results for gravity fingering to field soils and conditions, these and other complicating factors present in the field must be assessed. In the following sections, we give a cursory discussion and present several experiments that demonstrate fundamental effects on the fingering process induced by: the role of uniform and non-uniform initial moisture content; media heterogeneity; and the presence of large voids, such as macropores and fractures. Media hydraulic/capillary properties are discussed from a pore scale perspective elsewhere in this issue (Glass and Yarrington, 1996). These complicating factors may act to alter the expected scale of fingering, or entirely suppress its occurrence.

4.1. Uniform and non-uniform initial moisture content

In the field, we expect initial moisture contents to vary spatially and temporally. Only a limited amount of experimental data exists on the influence of initial moisture content on gravity fingering, most likely due to the difficulty of measuring and controlling initial moisture fields. However, the limited data available does imply that initial moisture content has a fundamental impact on finger behavior, and as such, warrants additional investigation.

The effects of uniform initial moisture content on finger development were explored in a series of experiments by Diment and Watson (1985) where instability of the wetting front after cessation of slug input was considered. They found that as the uniformly distributed initial moisture content increased, gravity fingering became less distinct. Glass et al. (1987) considered the generation of fingers from a point source under uniform dry and field capacity conditions using dyed water to delineate the growing wetted zones. Under dry initial conditions, a single finger formed from the point source that exhibited the saturated finger tip structure discussed previously. Under field capacity initial conditions, the wetting zone had the appearance of a wider, more diffuse “finger”. Recent experiments using the transmitted light moisture measurement technique (Fig. 7), however, shows the “finger” generated under field capacity initial conditions to be an expanding bulb that does not demonstrate the features of flow into dry sand where one narrow finger forms with a saturated tip that drains a distance behind.

Evidence such as this suggests that for uniform moisture contents where a connected network of filled pores and films exists, the dramatic finger structure exhibited in dry sands is suppressed. The upper limit of uniform initial moisture content for fingering to occur has not yet been determined and is difficult to explore experimentally. Diment and Watson (1985) chose to mix sand with a known amount of water and then pack the sand

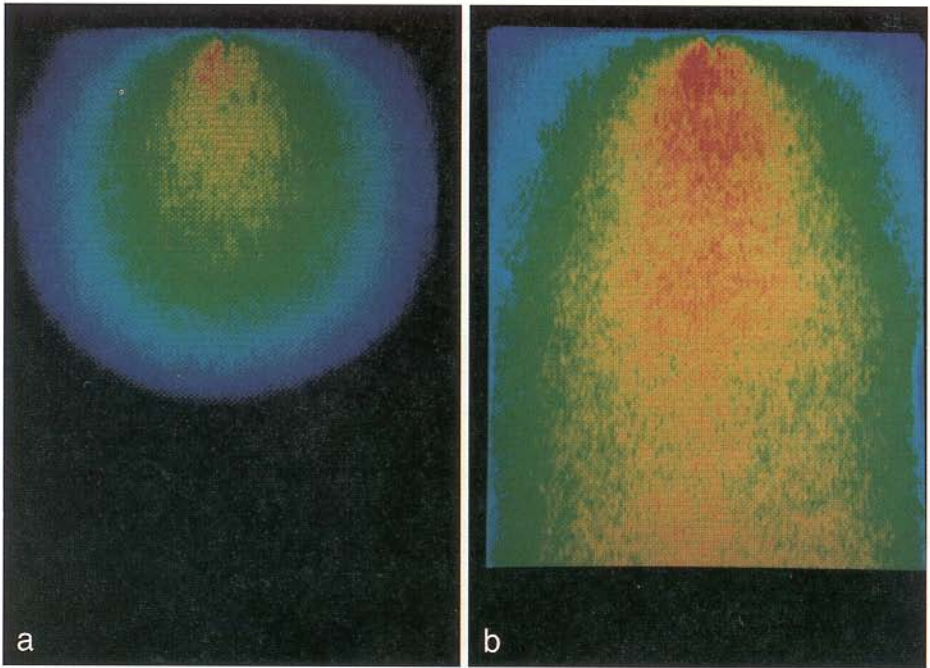


Fig. 7. Suppression of fingering due to residual initial moisture content. The developing (a) and final steady state (b) flow field for a point source buried 1 cm below the sand surface is elucidated using the light transmission technique in a slab of silica sand (1 cm thick, 25 cm wide, and 40 cm tall). The difference from initial conditions in the saturation field is represented with false color (black represents pre-infiltration residual moisture content and red near saturation).

into an experimental chamber. However, differences in packing under moist and dry conditions can be significant. A better approach, yet to be attempted, may be to equilibrate a single experimental packing with different water vapor pressures; thereby allowing the initial moisture content to be varied systematically without changing the micro geometry of the porous pack.

Non-uniform initial moisture content as formed by fingering in initially dry sand was studied by Glass et al. (1989d). They found that upon interruption of flow after the full development of the two-region core–fringe flow field, hysteresis in the pressure/saturation relation prevents the moisture content of the draining field from equilibrating to a uniform value. A subsequent infiltration event into the non-uniform initial moisture field shows the persistence of the finger flow structure from one infiltration event to the next (Fig. 8). The preferential flow features that form do not exhibit a saturated tip with drainage behind, as is seen under initially dry conditions. In addition, while the two zone moisture content field continues to dominate the flow field, the differences between the two zones are less distinct as demonstrated by solute transport experiments (Glass et al., 1989a).

Based on results in uniform moisture content fields at field capacity where fingering is suppressed (e.g. Fig. 8), the persistence of fingering cannot be due to instability in the

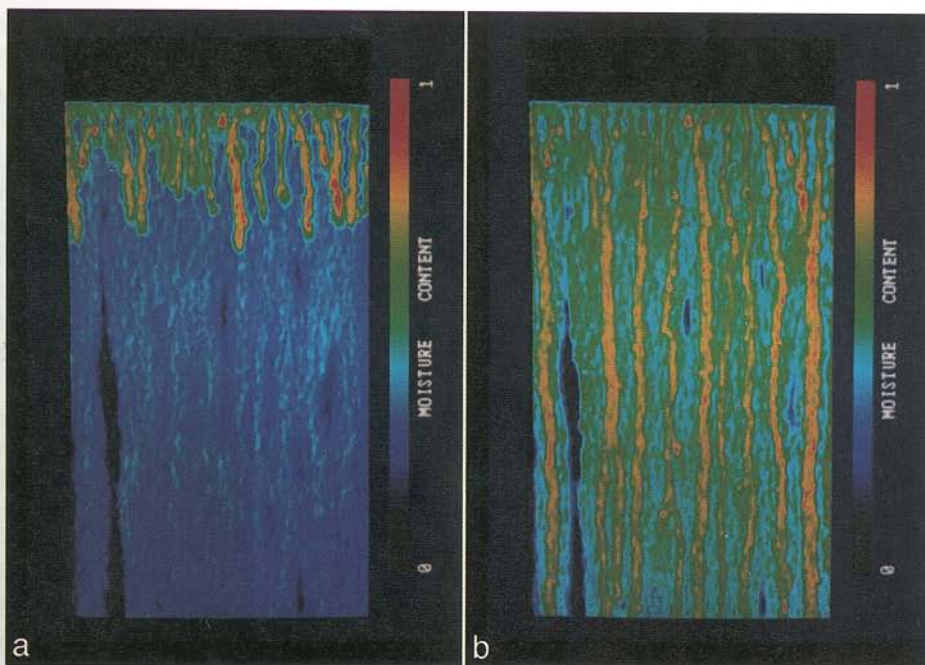


Fig. 8. Persistence of fingers in subsequent infiltration events. Following a 24 hour interruption of infiltration in the experiment of Figs. 1 and 3, during which time the lower layer drained, a subsequent infiltration event demonstrates the persistence of the core/fringe region structure during the rapid growth phase (a) and at steady-state (b) (from Glass et al., 1989d).

subsequent infiltration event. Indeed, the moisture contents present are high enough to stabilize even a point source at the top of the layer (Fig. 7). Instead, these fingers, while caused initially by an instability in dry sand, persist due to the combination of a heterogeneous initial condition and capillary hysteresis. Since the finger cores are initially wetter than the fringe regions, their permeability is higher than the fringe region at the same suction. The development of the two region moisture content field due to the initial instability has caused a homogeneous sand pack to behave subsequently as heterogeneous; the core and fringe regions having essentially different moisture characteristic curves.

The combined influence of initial moisture and hysteresis in the moisture characteristic curve to create persistent “fingers” within the vadose zone must not be overlooked. While these fingers may not be due to a gravity instability, the combination of gravity, non-uniformity of water supply (in time or space), and hysteresis can combine to form a flow field which contains heterogeneities in the moisture content field and persistent “fingers” rather than a homogeneous flow. Furthermore, long-term preferential flow along paths initiated by gravity fingering may lead to the formation of material heterogeneity through physio-chemical alteration, even in a uniform sand.

4.2. Media heterogeneity

The effect of slight within-layer media heterogeneity can be seen in all experiments reported to date that have used the method of Glass et al. (1989c) to fill and pack a “homogeneous” layer. Fig. 9 shows a transmitted light image of a dry experimental pack composed of 14–20 sand. The variation in the transmitted light field indicates the sand pack variability to be isotropic with a correlation length of about 1 cm. In these porous packs, both finger tip splitting and non-vertical finger movement or “meandering” are evident (see Fig. 1). Glass et al. (1989c) noted a relationship between meandering and flow rate supplied to individual fingers, the lower the flow rate supplied to the finger, the more local, small scale heterogeneities affected finger path. Examples of both low and high flow finger structures can be seen in Fig. 1.

The effect of meandering and flow rate in determining the final flow field structure within a two-layer steady flow experiment is also seen in Fig. 1. Many small, low flow fingers form at the flat textural interface as water moves into the higher permeability lower layer. These fingers meander and touch each other. When fingers touch, they tend to merge; the lower flow rate finger is sucked into the higher flow rate finger to form a wider, higher velocity finger that is less susceptible to local small scale heterogeneity.

The effect of moderate horizontal, within-layer media heterogeneity can be seen in the experiments of Hill and Parlange (1972), Pendexter and Furbish (1991), and the preliminary experiments of Glass et al. (1989c). In all these experiments, the experimenters attempted unsuccessfully to construct homogeneous layers. Small scale micro-

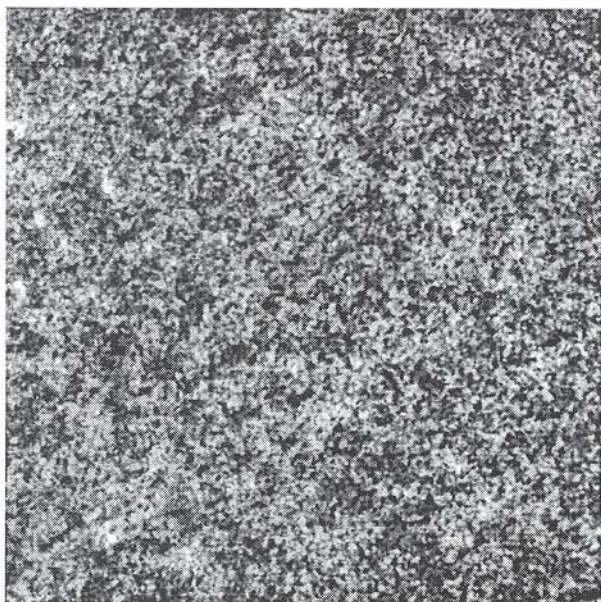


Fig. 9. Small scale heterogeneity within “homogeneous” sand pack. Light transmission technique is used to visualize heterogeneity within a 5 cm by 5 cm section of a 14–20 mesh sand slab.

layering within the experiment caused irregular finger edges and greater effective meandering producing a more convergent pattern and less fingers with depth.

In addition to within layer heterogeneity, heterogeneity along the textural interface is critical in determining where fingers will form at the top of a layer. Because of the contribution of the gravitational component to the total potential driving flow, water will most likely cross the textural interface at low points first. If the flow supplied to the system can be handled by these low points, only they will provide entry points to the lower layer. Hill and Parlange (1972) used this mechanism to trigger fingers at known locations. If imposed flow increases, additional fingers may form from the textural interface; however, in most field conditions, there are limits on the flow rates that occur naturally. Thus, heterogeneity along the interface effectively takes a uniform applied flow and distributes it among point and area sources from which fingers may then form.

In general, heterogeneities can be categorized as either flow divergence or convergence structures. Divergence structures are best exemplified by strong, pervasive media layering or micro-layering which increases capillary forces horizontally while decreasing permeability in the direction of gravity. Such structures are found in almost all subsurface alluvial deposits. Cross-bedding within alluvial deposits and finite length layers (lenses) of contrasting properties either horizontal or dipped are examples of convergence features. These structures are also found in almost all subsurface soils and unconsolidated sediments (see Fig. 5).

To demonstrate the effect of convergence and divergence structure media heterogeneity on gravity fingering, two experiments were conducted: the first incorporated within layer micro-layering and cross-bedding (Fig. 10) and the second micro-layering, cross-bedding, and an embedded layer of very fine sand (Fig. 11).

The first experiment used a single sand mixture (20–50 sieve fraction). The sand was added to the chamber through a funnel that was moved from point to point at the top of the chamber. Due to natural grading processes that occur as the falling sand hits the rising sand surface and rolls, either micro-layering or cross-bedding (analogous to that seen in subsurface alluvial deposits) results, depending on the position and movement of the funnel. Simple back and forth movement yields micro-layering, a divergence structure; the thickness of the micro-layers is a function of the frequency of the movement. A pause in the back and forth movement creates a sand pile directly under the funnel with sand rolling down, grading on its slopes, and forming a set of cross-beds. The intersection of two cross-bed sets creates a convergence structure.

A transmitted light image of the first experimental pack in the initial dry condition is shown in Fig. 10a. The standard color sequence reflects the raw light intensity with higher intensity (red) where the sand grains are larger and lower intensity (dark blue) where the grains are smaller. The bottom 20% of the pack is homogeneous where it was filled using a randomizer (Glass et al., 1989c). On top of the homogeneous layer, a convergent cross-bedding was embedded. At about the midpoint of the pack, cross-bedding graded into large amplitude micro-layering, then into small amplitude micro-layering. The top 20% of the chamber was filled using a randomizer to yield a homogeneous uppermost layer.

Water was supplied to the initially dry sand through two point sources at the top of the pack. Raw light intensity images of the advancing fingers are shown in Figs. 10b, c,

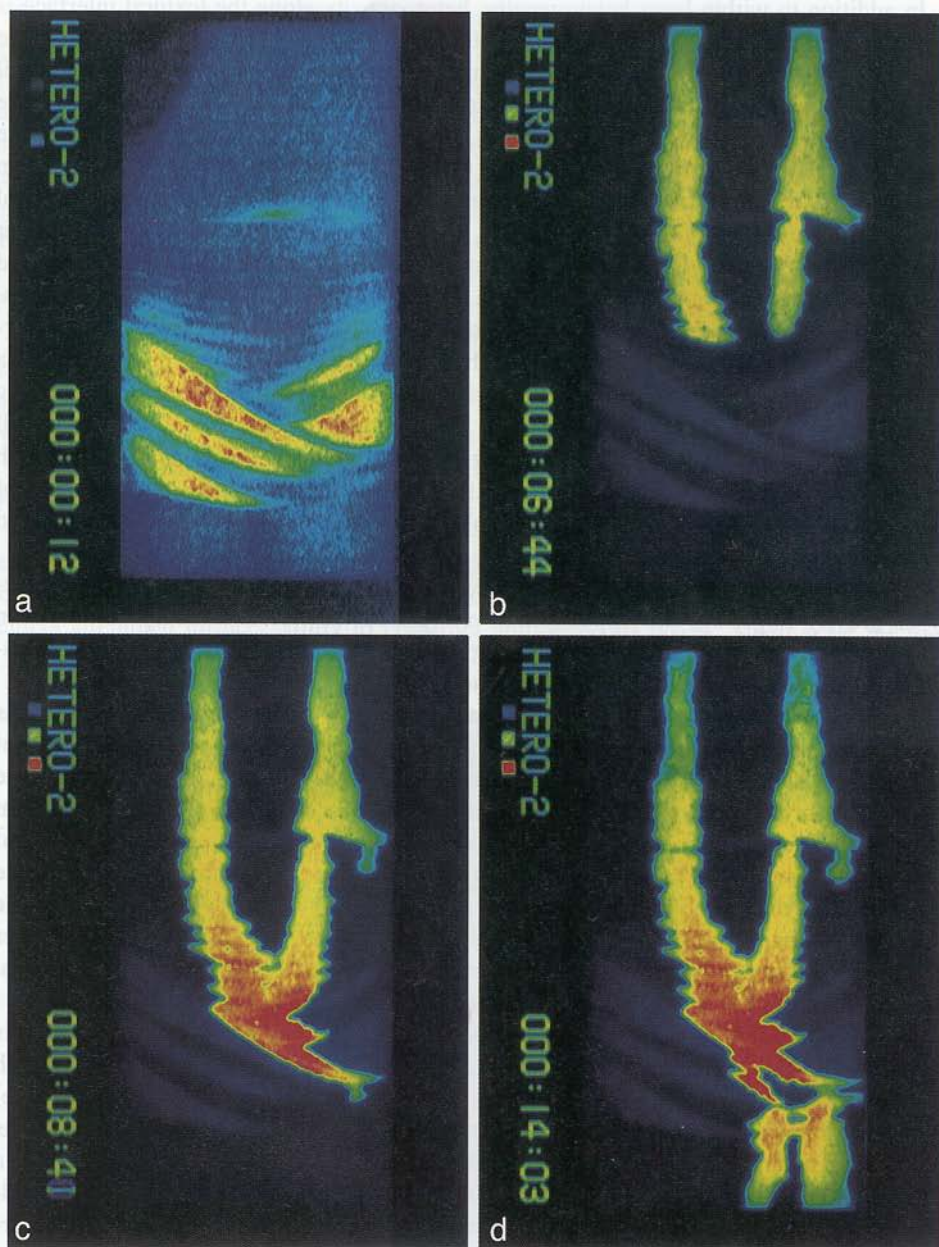


Fig. 10. Effect of micro-layering and cross-bedding heterogeneity. Light transmission technique is used to visualize heterogeneity in mean grain size within the sand pack, (a) (30 cm wide, 60 cm tall, and 1 cm thick). Cooler colors depict finer and hotter colors coarser zones. Water infiltration from two point sources is shown in (b), (c) and (d).

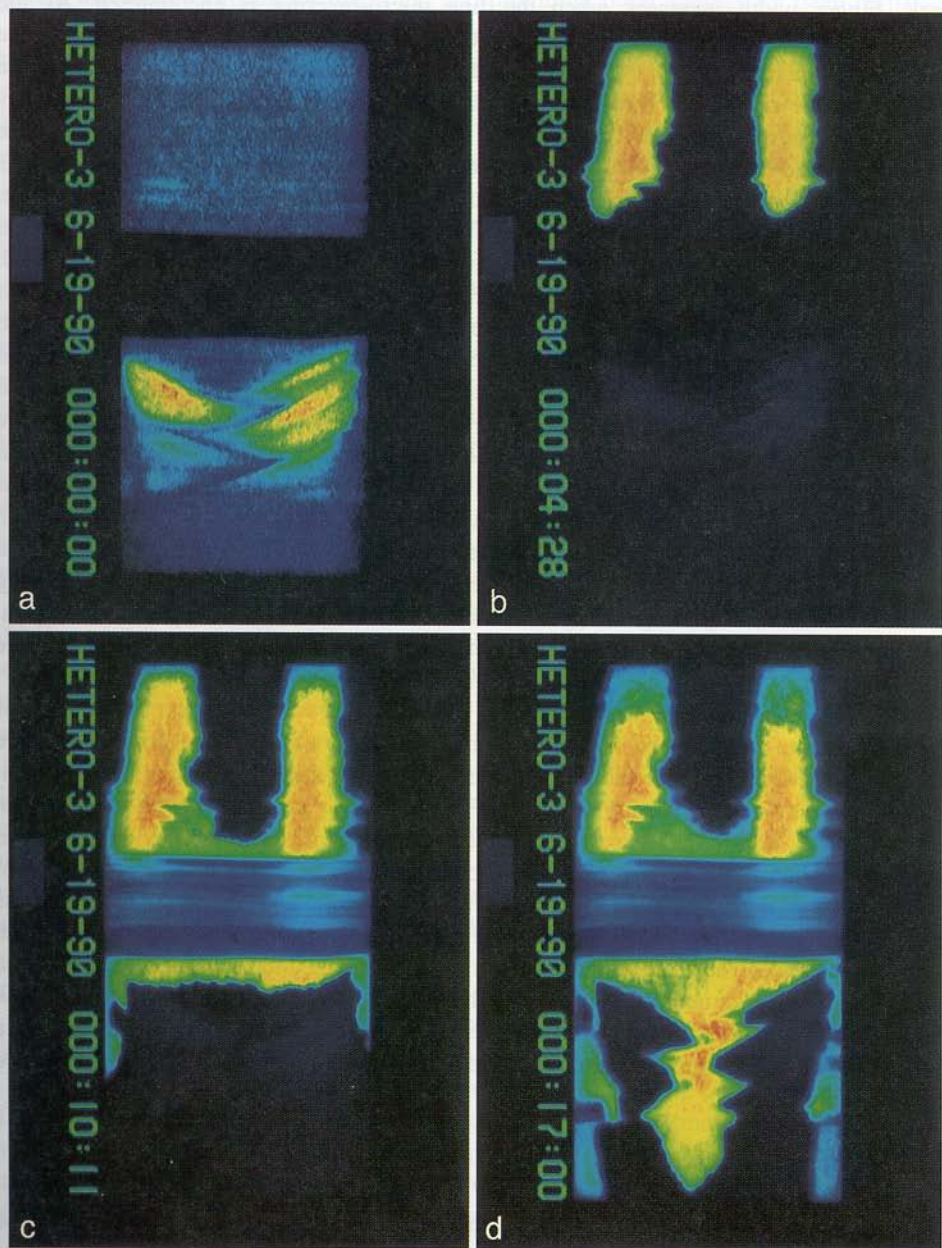


Fig. 11. Effect of embedded fine layer within micro-layering and cross-bedding heterogeneity. Light transmission technique is used to visualize heterogeneity in mean grain size within the sand pack, (a) (30 cm wide, 60 cm tall, and 1 cm thick). Cooler colors depict finer and hotter colors coarser zones. The black band midway down the sand pack denotes the embedded fine layer. Water infiltration from two point sources is shown in (b), (c), and (d).

and d. A finger forms below each point source in the homogeneous sand at the top of the pack. Finger width increases when the fine micro-layering is encountered. As the amplitude of the grain size variation within the micro-layering increases, the sides of the finger becomes more irregular. Note the effect of the small coarse zone two-thirds of the way up on the right-hand finger; the finger widens above the zone and then narrows below. The converging cross-bedding unit causes the merger of the two fingers. The influence of the large grain layers within the unit as capillary barriers that focus flow is clearly evident in Fig. 10c. Once through the cross-bedded unit, fingers emanate from each point of supply. Note that a small finger broke through the major coarse cross-bedded unit causing the initially merged flow field to again split apart (Fig. 10d). Also note that the finger cores at the top of the experiment do not begin to exhibit desaturation until the finger tips are near the bottom of the chamber as seen in Fig. 10d.

In the second experiment, the same sequence of units was emplaced with the addition of a fine (100–140 mesh), micro-layered unit inserted directly above the cross-bedded unit (see Fig. 11a, black unit is the inserted fine layer). Flow again was instigated to the dry pack from two point sources at a rate approximately 40% higher than the first experiment (Fig. 11b, c, d). Notice that, as expected, the fingers begin wider and show less widening as the micro-layered zone on top of the fine unit is encountered. Within the fine micro-layered unit, the fingers immediately merge and the system is stabilized at the scale of the experiment. Once the wetting front has moved into the underlying cross-bedded unit, fingers again appear which follow the finer cross-layers. Once again, notice that the finger cores at the top of the experiment have not begun to desaturate until Fig. 11d.

In all the laboratory examples discussed above, if fingers could form at the scale of the experiment, the effect of within layer heterogeneity was to cause greater effective meandering, merger, and the tendency to focus flow with depth to stronger, less frequent fingers that carry an increasing amount of the flow. In combination with the fact that non-horizontal, non-uniform textural interfaces break any pattern that may have resulted from the fundamental hydrodynamic instability process at a flat interface, the use of system level equations derived for finger size and spacing from linear stability analysis in field situations is far from tenable. Where gravity fingering may occur in the field, convergence and divergence structures must be characterized in terms of size and spatial correlation. These structures themselves should define finger location size and flow rates. Thus, from the soil surface, a pattern of fingers evolves with depth that is a function of the flow rate through the system and the strength and type of subsurface heterogeneity present.

4.3. Macropores / fractures

Large connected void spaces within the porous media, such as macropores and fractures are expected to have a fundamental impact on gravity fingering. Macropores are found in many soils and sub-soils and are typically of organic origin, including, but not limited to worm holes, animal burrows, and decayed root channels. Fractures are planar stress features which occur in many stiff soils and in virtually all near surface rock units. These relatively large void spaces can impact the development of fingers

through at least three means: acting as capillary barriers to flow; forming a separate flow system that is also capable of fingering; and providing point sources for deep recharge.

Under unsaturated conditions, large void spaces are expected to act as capillary barriers to flow. Such features will tend to guide flow through the system. With respect to the bounding geometric cases, vertically oriented features would constrain lateral finger movement, while horizontal features would induce lateral spreading. Consider as an example, orthogonal sets of vertically oriented fractures, which would be expected to constrain flow within the soil matrix much in the way of a laboratory column. If the horizontal length scale imposed by the bounding fractures is less than the expected finger width in the matrix, stable wetting front advancement will be induced.

Although large voids normally provide capillary barriers to matrix flow, in numerous situations, both at the surface and at depth, flow may occur within the macropores or fractures themselves. Flow through large voids may initiate from flux rates greater than matrix capacity (ponded infiltration) or where local heterogeneity provides a direct feed. Once flow has initiated, low sorptivity into the adjacent matrix may allow flow through the large void spaces and subsequent fingering in non-horizontal features. Such low sorptivity would be expected in stiff fractured soils, and may also result from physiochemical alteration along the walls of large void spaces in granular soils. Gravity fingering is expected to occur in tubes above a diameter defined by capillary properties of the system and at flux rates less than saturated flux.

Vertical bands of solute observed in field investigation of fractured clays (Dekker, 1994), and fractured tuffaceous rock (Nicholl et al., 1994) provide evidence for the occurrence of fingering in near surface fractures under field conditions. Within fractures, recent experiments have explored gravity fingering and demonstrated both similarities and dissimilarities to observed behavior in porous media (Nicholl et al., 1992, 1993a,b,1994). Similarities include situations that are unstable, relationships between finger velocity and width, and moisture content structure of individual fingers within initially dry fractures (Fig. 12). The major dissimilarity is the effect of uniform initial moisture content; in porous media gravity fingering is suppressed by uniform initial moisture content, while in fractures it is enhanced (Fig. 13). In addition, observations of nonsteady flow structures within individual fingers supplied with fluid under steady conditions raise the question of whether gravity flow in fractures has a chaotic component (Fig. 14).

As previously discussed, fingers are observed in the laboratory to initiate from localized preferential flow at material interfaces. Flow through large void spaces within a soil layer may act as a focusing mechanism capable of forming point sources at depth. If flux through the large void feature is less than K_s of the material at its terminus, gravity fingers would be expected to develop. If flux is greater than K_s of the terminal material, fluid may back-up within the large void, forming a ponded condition; cessation of ponded inflow is then capable of inducing gravity fingers.

5. Gravity fingering and NAPL movement

The subsurface movement of non-aqueous-phase liquids (NAPLs) from surface spills and landfills is an area of increasing concern within vadose and saturated zone

contaminant hydrology. NAPLs are differentiated into two classes on the basis of density. LNAPLs such as gasoline are lighter than water while DNAPLs such as TCE and PCE are denser. The previously discussed stability criterion (Eq. 1) and relations for minimum finger width (d_c , Eqs. 3 and 4) may apply to the development of gravity fingering in systems composed of NAPL/air and NAPL/water. However, these equations have yet to be tested and for the NAPL/water/air system present in the vadose zone, no stability criteria or predicted minimum finger widths have yet been formulated.

An image sequence collected from an experiment in an initially air saturated two-layer, fine sand over coarse experiment comparable to that shown in Fig. 1 is shown in Fig. 15. Oil was “spilled” on the top layer where it then evenly infiltrates, implying stability at the system width. As the NAPL front crossed the textural interface, wide fingers formed and moved downward through the bottom layer. The fingers exhibited saturated tips that drained a distance behind. On a qualitative basis, observed behavior is consistent with that of water-over-air systems; however, the finger widths, velocities, and saturated tip lengths were distinctly different, as expected from the difference in fluid and capillary properties between NAPL/air and water/air systems (see Eqs. 18 and 19).

Drainage of the experiment (air invasion) following cessation of the “spill” resulted in an oil saturated top fine layer overlying a coarse lower layer containing an oil

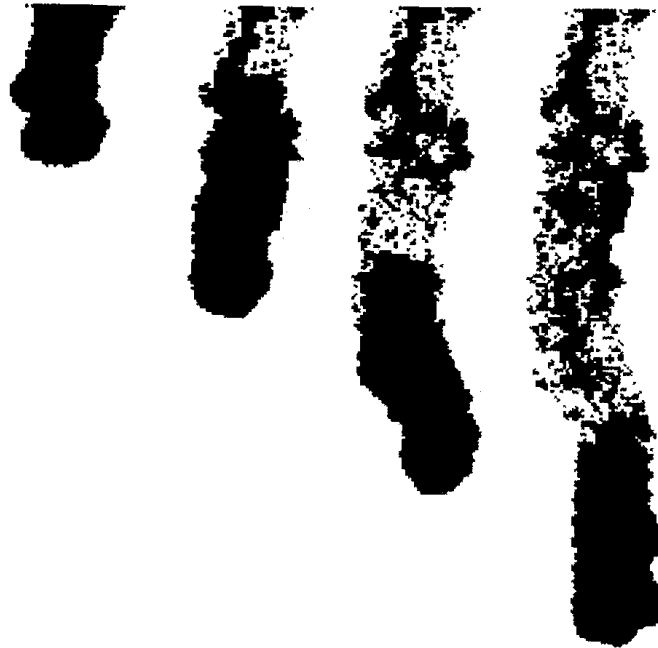


Fig. 12. Finger development in an initially dry fracture. Steady flow to a point source on the upper boundary of a dry, rough-walled analog fracture (Nicholl et al., 1993a) leads to fingering behavior analogous to that observed in porous media. The finger first develops as a hanging column, held to the upper boundary by capillary forces (left). As the column lengthens, it applies increasing suction at the upper boundary. When applied suction becomes sufficient to overcome air-entry pressure, the hanging column breaks free and moves as a unit (middle left); a desaturated region may then develop behind the advancing finger tip (middle and far right).

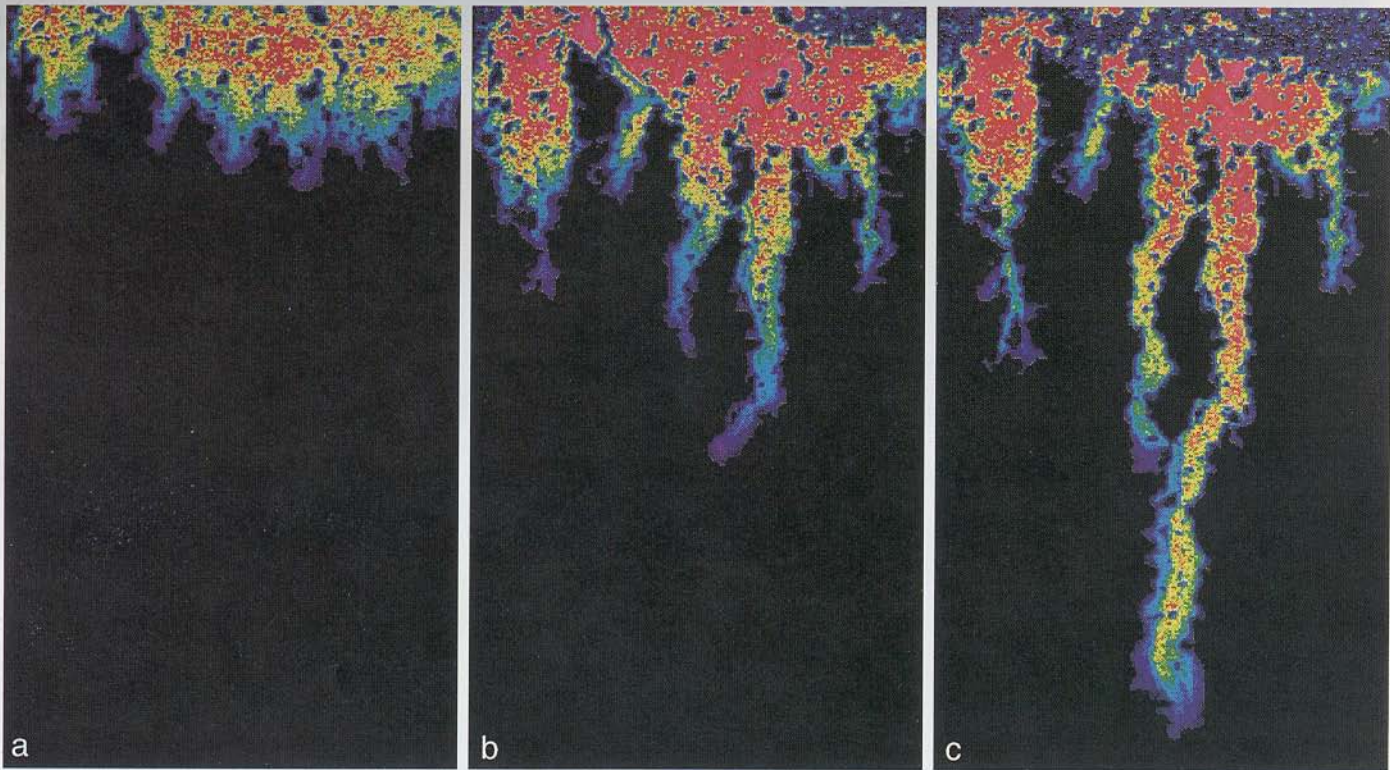


Fig. 13. Gravity fingers in a uniform moisture field. Nicholl et al. (1993b) reported that contrary to studies in porous media, prewetting an inclined, analog fracture to field capacity destabilized, rather than stabilized, infiltration. Here, the cessation of ponded infiltration results in the formation of complex gravity fingering structures in a prewetted analog fracture (30×60 cm).

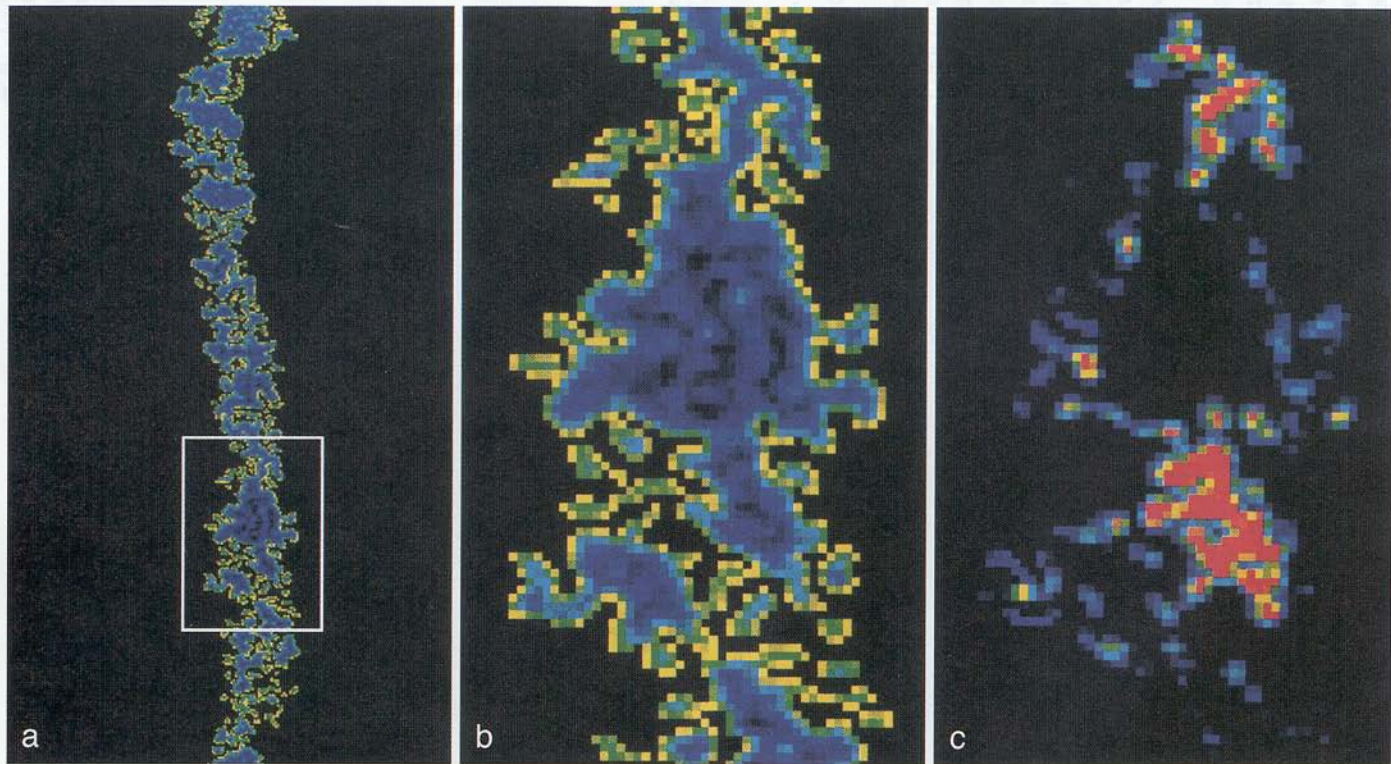


Fig. 14. Unsteady and possibly chaotic flow regimes. In an initially dry, inclined, analog fracture (15×30 cm) steady supply at less than the saturated conductivity leads to fingering (Nicholl et al., 1993a). At steep inclinations and small flow rates, fluid within the desaturated zone behind the finger tip was observed to be concentrated in a series of small, intermittently connected "reservoirs" (a and b). The right-hand image (c) illustrates system dynamics for the reservoir seen in the center image; the reservoir contracts and expands (blue outline) and repeatedly disconnects from adjacent features (red/green). Such behavior has strong analogies to the classic "dripping faucet" example of chaotic flow.

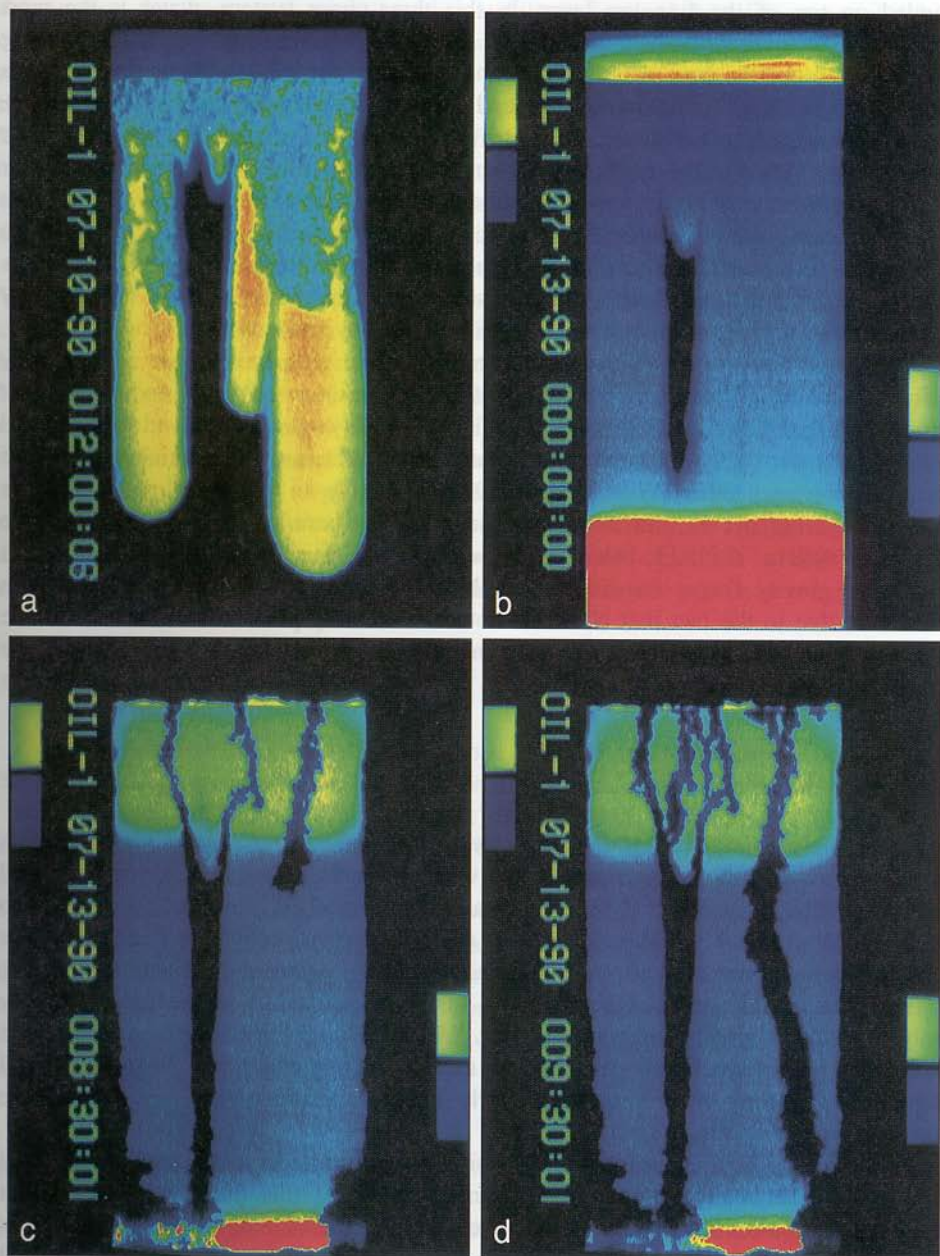


Fig. 15. NAPL fingering in a two-layer system. A series of images showing oil (NAPL) infiltration, (a), followed by oil drainage to the static condition, (b), followed by water infiltration, (c) and (d), into a two-layered fine over coarse, initially dry sand system similar to that shown in Fig. 1 (30 cm wide, 60 cm tall, and 1 cm thick). Oil is visualized as hotter colors in the images. Infiltrating water is seen in (c) and (d) as the growing dark regions.

saturated zone at the bottom (Fig. 15b). Water dyed with FD and C blue #3 was then ponded on top of the fine top layer. In this three-phase system, water is the most wetting, oil is of intermediate wettability, and air is the non-wetting fluid. Imbibing water pushed out the less wetting, less dense oil from the oil saturated top layer in a stable configuration (here viscous and capillary stability outweighs density instability). Upon entering the bottom layer, the water formed gravity fingers through the oil/air system (Fig. 15c, d). These fingers were narrower where the oil content was higher directly beneath the top layer and wider where the oil content decreased below. When a zone without oil was encountered, as can be seen in a vertical zone in the middle of the experiment, the water finger moved preferentially into and through the zone. This occurs due to the combination of wettability considerations (the water strongly wets the dry porous media) and the local balance of capillary, gravity, and viscous forces.

The complicated nature of the dual fingering within such three-phase systems may make prediction of NAPL movement within the unsaturated zone and subsequent remediation based on forced flows very difficult. Stability criterion derived for two-fluid systems are most likely not applicable to three-phase systems. Differential spreading of the phases on each other (Wilson et al., 1990) may play an important role in whether gravity fingering occurs and its scale of expression (pore or macroscopic). For the two-phase system, if NAPL behaves like water in the sense that initial liquid content suppresses gravity finger formation, then NAPL fingering may be significant in the subsurface due to the fact that NAPL is not often initially present. For DNAPL in the saturated zone, fingering may be further enhanced because many DNAPLs tend to be less viscous than water.

6. Conclusion

Linear analysis implies that clear cut rules exist for the occurrence of gravity fingers during downward infiltration of water into water wettable soils. However, as discussed here, the assumptions inherent in linear analysis are somewhat limiting with respect to field conditions. Real world soils contain a plethora of complicating factors that are expected to fundamentally effect, and perhaps entirely suppress the fingering process. To demonstrate this point, a simple field test was performed where linear stability analysis predicted gravity fingering to occur. While dye tracer fronts showed evidence of preferential paths (small scale perturbations that show no inclination to form full fledged fingers), the wetting front showed a nearly uniform spatial distribution without the formation of gravity fingers.

Results of this field experiment underscore the need to understand conditions in field soils that fundamentally effect the fingering process. At this time, it is known that uniform and non-uniform initial moisture content, media heterogeneity, and the existence of large void spaces such as macropores and fractures can have fundamental effects on the fingering process. Initial moisture content, in general, is found to stabilize the flow field; however, if it is distributed non-uniformly, fingered flow is observed to combine with hysteresis to create a heterogeneous permeability field such that subsequent events follow preferential flow paths defined by previous fingers. Media hetero-

geneity can be classified into flow convergence or divergence structures. Experiments demonstrate that horizontal micro-layering stabilizes fingered flow (divergence), while cross-bedding acts to concentrate and coalesce fingers (convergence). Networks of macropores/fractures can act as a separate “media” that can both constrain flow within the matrix to be stable and allow instability to form within the high permeability media. Our consideration of each of these is far from complete. However, due to these and other complicating factors, it is unlikely that the results from linear stability theory will be relevant for predicting finger occurrence, size, number, spacing, or cross-sectional area open to flow except under extremely simple conditions (e.g., engineered systems).

Numerical analysis, both at the pore and the continuum scale (e.g., Glass and Yarrington, 1996; Nieber, 1996) shows considerable promise for considering both the complicating factors discussed above and the effects of hydraulic/capillary properties by systematic parameter variation that is not feasible in the laboratory. This ability may be particularly useful for considering interfacial instability occurring during either the emplacement or remediation of non-aqueous phase liquids (NAPLs). The simple experiment we present to simulate a NAPL spill on dry sands followed by water infiltration suggests gravity fingering to play a significant role in this parallel system relevant to many sites of industrial contamination. Whereas initial moisture content is ubiquitous and acts as a suppressing agent in air/water systems, the lack of NAPL in the subsurface may act to accentuate the fingering process in real soils and subsoils.

Acknowledgements

Many people have contributed to the work summarized in this paper: Lee Orear of Sandia National Laboratories and Craig Ginn of Spectra Research helped to conduct the “heterogeneous”, “initial moisture content” and “NAPL” experiments in 1990; Jim Brainard, Carl Martin, Drew Baird, Dan Garrett, and Bob Holt helped design and conduct the field experiment as part of the 1992 Vadose Zone Hydrology Class taught by the senior author at the University of New Mexico; Huy Nguyen of the University of New Mexico helped to conduct the experiments in fractures in 1992; Mehdi Eliassi of the University of New Mexico and Dennis Norton of the University of Arizona calculated the hysteretic moisture retention curve presented in Fig. 2. Thoughtful reviews of the manuscript were given by Steven Conrad, Steven Webb, and Peter Davies of Sandia National Laboratories.

References

- Baker, R.S. and Hillel, D., 1990. Laboratory tests of a theory of fingering during infiltration into layered soils. *Soil Sci. Soc. Am. J.*, 54: 20–30.
- Chouke, R.L., Van Meurs, P. and Van der Poel, C., 1959. The instability of slow immiscible, viscous liquid–liquid displacements in porous media. *Trans. Am. Inst. Min. Eng.*, 216: T.P.8073.
- Dekker, L., 1994. Moisture patterns in field soils. Presentation at the Symposium on Fingered flow in Unsaturated Soil: From Field to Model. Winand Staring Centre, Wageningen, The Netherlands, April 20, 1994.

- Diment, G.A. and K.K. Watson, 1985. Stability analysis of water movement in unsaturated porous materials. 3. Experimental Studies. *Water Resour. Res.*, 21: 979–984.
- Glass, R.J., 1992. Miller scaling of finger properties in sandy soils: An indirect method for estimating finger width and velocity. In: M.T. van Genuchten (Editor), *Indirect Methods for Estimating the Hydraulic Properties of Unsaturated Soils*, pp. 533–569.
- Glass, R.J. and Yarrington, L., 1996. Simulation of gravity fingering in porous media using a modified invasion percolation model. *Geoderma*, 70: 231–252, this issue.
- Glass, R.J., Parlange J.-Y. and Steenhuis, T.S., 1987. Water infiltration in layered soils where a fine textured layer overlays a coarse sand. *Proc. Int. Conf. for Infiltration Development and Application*, Honolulu, HI, Jan. 5–9, 1987, pp. 66–81.
- Glass, R.J., Oosting, G.H. and Steenhuis, T.S., 1989a. Preferential solute transport in layered homogeneous sands as a consequence of wetting front instability. *J. Hydrol.*, 110: 87–105.
- Glass, R.J., Parlange, J.-Y. and Steenhuis, T.S., 1989b. Wetting front instability I: Theoretical discussion and dimensional analysis. *Water Resour. Res.*, 25: 1187–1194.
- Glass, R.J., Steenhuis, T.S. and Parlange, J.-Y., 1989c. Wetting front instability II: Experimental determination of relationships between system parameters and two dimensional unstable flow field behavior in initially dry porous media. *Water Resour. Res.*, 25: 1195–1207.
- Glass, R.J., Steenhuis, T.S. and Parlange, J.-Y., 1989d. Mechanism for finger persistence in homogeneous unsaturated porous media: Theory and verification. *Soil Sci.*, 148: 60–70.
- Glass, R.J., King, J., Cann, S., Steenhuis, T.S. and Parlange, J.-Y., 1990. Wetting front instability in unsaturated porous media: A three-dimensional study in initially dry sand. *Transp. Porous Media*, 5(3): 247–268.
- Glass, R.J., Orear, L., Ginn, W.C., Parlange, J.-Y. and Steenhuis, T.S., 1991a. Miller scaling of finger properties. Presentation at the Workshop on the Characterization of Transport Phenomena in the Vadose Zone. University of Arizona, April 2–5, 1991.
- Glass, R.J., Parlange, J.-Y. and Steenhuis, T.S., 1991b. Two-phase immiscible displacement in porous media: Stability analysis of three-dimensional, axisymmetric disturbances. *Water Resour. Res.*, 27: 1947–1956.
- Hill, D.E. and Parlange, J.-Y., 1972. Wetting front instability in layered soils. *Soil Sci. Soc. Am. Proc.*, 36: 697–702.
- Hogarth, W.L., Hopmans, J., Parlange, J.-Y. and Haverkamp, R., 1988. Application of a simple soil-water hysteresis model. *J. Hydrol.*, 98: 21–29.
- Liu, Y., Steenhuis, T.S., Parlange, J.-Y. and Selker, J.S., 1991. Hysteretic finger phenomena in dry and wetted sand. In: T.J. Gish and A. Shirmohammadi (Editors) *Preferential Flow: Proc. of the National Symposium*. *Am. Soc. Agric. Eng.*, pp. 160–172.
- Martin, K.A., Baird, D.C. and Glass, R.J., 1993. Infiltration into thick unsaturated alluvial deposits: A preliminary study. In: *Proc. 1993 Natl. Conf. on Hydraulic Engineering and International Symposium on Engineering Hydrology*, San Francisco, CA, July 25–30, 1993. *Engineering Hydrology Volume*, pp. 174–179.
- Miller, E.E. and Miller, R.D., 1956. Physical theory for capillary flow phenomena. *J. Appl. Phys.*, 27: 324–332.
- Nicholl, M.J., Glass, R.J. and Nguyen, H.A., 1992. Gravity-driven fingering in unsaturated fractures. *Proc. 3rd Int. Conf. of High Level Rad. Waste Manage.* American Nuclear Society, pp. 321–331.
- Nicholl, M.J., Glass, R.J. and Nguyen, H.A., 1993a. Small-scale behavior of single fingers in an initially dry fracture. *Proc. 4th Int. Conf. of High Level Rad. Waste Manage.*, American Nuclear Society, pp. 2023–2032.
- Nicholl, M.J., Glass, R.J. and Nguyen, H.A., 1993b. Wetting front instability in initially wet fractures. *Proc. 4th Int. Conf. of High Level Rad. Waste Manage.*, American Nuclear Society, pp. 2061–2070.
- Nicholl, M.J., R.J. Glass and S.W. Wheatcraft, 1994. Gravity-driven infiltration instability in initially dry non-horizontal fractures. *Water Resour. Res.*, 30(9): 2533–2546.
- Nieber, J.L., 1996. Modeling finger development and persistence in unsaturated porous media. *Geoderma*, 70: 207–229, this issue.
- Palmquist, W.N. and Johnson, A.I., 1960. Model study of infiltration into layered materials. *Am. Soc. of Civil Engin. Annual Meeting*, Boston, MA. October 10–14, 1960.

- Palmquist, W.N. and Johnson, A.I., 1962. Vadose zone in layered and non layered materials. Geological Survey Res. Article 119, c142–143.
- Parlange, J.-Y. and Hill, D.E., 1976. Theoretical analysis of wetting front instability in soils. *Soil Sci.*, 122: 236–239.
- Parlange, J.-Y., Glass, R.J. and Steenhuis, T.S., 1990. Application of scaling to the analysis of unstable flow phenomena. In: D. Hillel and D.E. Elrich (Editors), *Scaling in Soil Physics: Principles and Applications*. Soil Science Society of America, Madison, WI, pp. 53–58.
- Peck, A.J., 1965. Moisture profile development and air compression during water uptake by bounded porous bodies: 3 vertical columns. *Soil Sci.*, 100: 44–51.
- Pendexter, W.S. and Furbish, D.J., 1991. Development of a heterogeneous moisture distribution and its influence on the evolution of preferred pathways of flow in an unsaturated sandy soil. In: T.J. Gish and A. Shirmohammadi (Editors), *Preferential Flow: Proceedings of the National Symposium*. Am. Soc. Agric. Eng., pp. 104–112.
- Saffman, P.G. and Taylor, G.I., 1958. The penetration of a fluid into a porous medium or Hele–Shaw cell containing a more viscous liquid. *Proc. R. Soc. Lond.*, A245: 312–331.
- Selker, J.S., Leclercq, P., Parlange, J.-Y. and Steenhuis, T.S., 1992a. Fingering flow in two dimensions 1. Measurement of matric potential. *Water Resour. Res.*, 28: 2513–2521.
- Selker, J.-Y. Parlange and Steenhuis, T.S., 1992b. Fingering flow in two dimensions 2. Predicting finger moisture profile. *Water Resour. Res.*, 28: 2523–2528.
- Selker, J.S., Steenhuis, T.S. and Parlange, J.-Y., 1992c. Wetting front instability in homogeneous sandy soils under continuous infiltration. *Soil Sci. Soc. Am. J.*, 56: 1346–1350.
- Tabuchi, T., 1961. Infiltration and ensuing percolation in columns of layered glass particles packed in laboratory. *Nogyo doboku kenkyu, Bessatsu (Trans. Agric. Eng. Soc., Japan) 1*: 13–19.
- Tidwell, V.C. and Glass, R.J., 1994. X-ray and visible light transmission for laboratory measurement of two-dimensional, saturation fields in thin slab systems. *Water Resour. Res.*, 30(11): 2873–2882.
- Wilson, J.L., Conrad, S.H., Mason, W.R., Peplinski, W. and Hagan, E., 1990. Laboratory investigation of residual liquid organics from spills, leaks, and the disposal of hazardous wastes in groundwater. EPA/600/6-90/004, April 1990.